

# Influence of Electron and Ion Thermodynamics on the Magnetic Nozzle Plasma Expansion

IEPC-2013-247

Presented at the 33<sup>rd</sup> International Electric Propulsion Conference,  
The George Washington University, Washington, D.C., USA  
October 6–10, 2013

Mario Merino\* and Eduardo Ahedo†

Universidad Carlos III de Madrid, Avda. de la Universidad 30, 28911 Leganés (Madrid), Spain

**A two-fluid, two-dimensional model of the supersonic plasma flow in a divergent magnetic nozzle is extended to include different thermodynamic behaviors for electrons and ions. The effects of electron cooling under a polytropic law are studied, showing that the earlier hypersonic jet associated with cooling results in a lower beam divergence and facilitates plasma detachment. Ion thermal energy is converted to directed kinetic energy by the gasdynamic acceleration mechanism without the mediation of an ambipolar electric field, and alters the electric response of the plasma. Further work to include anisotropic and kinetic effects is outlined.**

## I. Introduction

A magnetic nozzle (MN) is an applied convergent-divergent magnetic field capable of guiding the expansion of an energetic plasma jet and accelerating it supersonically into vacuum. The *contactless* operation of MNs avoids the detrimental durability and efficiency issues associated to plasma-wall interactions, and provides a superior control over the expansion. These qualities make them an interesting device to produce thrust in space. Currently, several advanced plasma thrusters, including the Helicon Plasma Thruster<sup>1–4</sup> (HPT), the Electron Cyclotron Resonance Thruster<sup>5</sup> (ECRT), the Applied-Field MagnetoPlasmaDynamic thruster<sup>6–8</sup> (AF-MPD), and the VASIMR,<sup>9</sup> employ a MN as their main acceleration stage.

In a MN, the internal energy of the plasma is transformed into directed kinetic energy, much like in the case of a neutral gas in a traditional, solid de Laval nozzle. Therefore, all plasma thrusters operating on a MN are, in essence, thermal rockets: this means that specific impulse is roughly proportional to the square root of the temperature to which the plasma is heated inside the plasma source over the ion mass, i.e.,  $I_{sp} \propto \sqrt{T/m_i}$ , requiring very large temperatures (tens to hundreds of eV) to achieve competitive  $I_{sp}$  with usual propellants like Argon or Xenon. Notwithstanding, MNs (and the plasma thrusters relying on them) constitute an attractive propulsive technology thanks to their higher thrust-to-power ratio, simplicity, robustness, versatility, and presumed long useful life. As an example, consider the HPT, which consists merely of a quartz tube wrapped by a helicon antenna, into which the propellant is injected, a RF power source, and a few solenoids or permanent magnets that create the necessary magnetic field;<sup>10</sup> it can in principle be fed with multiple gases; and has no naked electrodes (which are the critical life limiting element in traditional plasma thrusters). Additionally, MNs bring up the interesting possibility of an enhanced ‘throttleability’, i.e., the ability of adapting in-flight the specific impulse and thrust of the device by modifying the massflow, applied power, and the intensity and geometry of the magnetic field.

In contrast to a solid nozzle, which has a physical wall on where the propellant exerts a pressure force to produce thrust, the more complex physics of a plasma flowing in a MN give rise to a variety of *acceleration mechanisms*, not present in a solid nozzle, which involve (i) azimuthal, diamagnetic electric currents in the plasma and the magnetic force on them, (ii) the development of an ambipolar electric field that transforms electron energy into ion energy, (iii) the possible formation of electric double layers within the plasma flow,

---

\*mario.merino@uc3m.es, aero.uc3m.es/ep2

†Professor, eduardo.ahedo@uc3m.es

(*iv*) the plasma-induced magnetic field, and (*v*) the form in which the internal energy is stored in the plasma (i.e., the particularities of the energy distribution function of each species). Additionally, the closed nature of the magnetic lines, opposed to the finite length of a solid nozzle, raises the question of efficient plasma detachment from the field to form a free plume downstream (an issue not present in ground applications of MNs such as advanced plasma treatments of material surfaces). Without proper detachment, the plasma would instead turn back along the magnetic streamlines, ruining thrust and endangering the spacecraft.

Current understanding of MN physical phenomena is limited to the few existing experiments, normally linked to particular plasma thruster prototypes, and models of the plasma flow in the magnetic field. As relevant examples, the experiments of Andersen *et al.*,<sup>11</sup> Kuriki *et al.*,<sup>12</sup> York *et al.*<sup>13</sup> and Inutake *et al.*<sup>14</sup> demonstrate the basic operation of the MN, including the supersonic acceleration of the ion flow, and the existence of the ambipolar acceleration mechanism. These developments were accompanied by several theoretical developments, mainly based on simple 1D models, 2D models or single-particle models, such as those of Kosmahl,<sup>15</sup> Chubb,<sup>16</sup> Gerwin *et al.*,<sup>17</sup> Sercel<sup>18</sup> and Mikellides *et al.*<sup>19</sup> Some of these models, however, rely upon two assumptions which have proven to be inadequate for the study of MNs: first, the use of a basic Ohm's law that ignores Hall and pressure terms completely (to first order, the *difference* between these two terms governs the development of the electric field), and second, the imposition of strong current ambipolarity (that is, ions and electrons are forced to expand identically, forbidding any internal separation of the two flows). Aiming to overcome these shortcomings, Ahedo and Merino<sup>20</sup> formulated a two-dimensional, two-fluid model that was then used to illustrate the main acceleration mechanisms in a hot-electron cold-ion plasma, and showed that the thrust generated by the MN is the magnetic reaction force caused by the diamagnetic plasma currents on the MN generator. The diamagnetic nature of the plasma currents was observed by Roberson *et al.*,<sup>21</sup> and the magnetic character of thrust was later confirmed by Takahashi *et al.*<sup>22</sup> In a comprehensive report, Gerwin<sup>23</sup> investigates the role of anomalous resistivity and plasma instabilities in MNs based on a 1D model, and proposes the application of extra magnetic coils further downstream to better control the plasma flow and improve plasma detachment.

In the last two decades, much of the MN-related work has focused on the study of plasma detachment. Experiments by Cox *et al.*,<sup>24</sup> Deline *et al.*,<sup>25</sup> Terasaka *et al.*,<sup>26</sup> Squire *et al.*,<sup>27</sup> and Takahashi *et al.*<sup>28</sup> all show that detachment begins to take place, to some extent, in the near-region (i.e., up to a few plasma radii away from the thruster exit). Notwithstanding, a successful explanation of this phenomenon remains to be found: models by Moses *et al.*,<sup>29</sup> Hooper<sup>30</sup> and Arefiev *et al.*<sup>31</sup> propose different separation mechanisms, based on different types of MHD cold-plasma models; these mechanisms, however, have been shown to be inadequate for a propulsive MN,<sup>32,33</sup> where the cold-plasma assumption is incompatible with the thermal-nature of these devices. Moreover, a complete theory that robustly includes plasma detachment in the far-region (once most acceleration has taken place and magnetic lines start to turn around) and a downstream closure of the plasma expansion is still lacking. The reason for this lays in the formidable difficulties involved in studying the far-region plume, both with experiments, where vacuum requirements to avoid plasma-ambient interaction are too high for laboratory tests and very large chambers are needed, and in the modeling/simulation realm, where phenomena like demagnetization, resistivity, population anisotropization, thermodynamic behavior of each species, interaction with an ambient plasma or an external magnetic field, and non-neutral effects associated to the very low densities are no longer negligible and have to be considered. A preliminary analysis<sup>34</sup> without these effects shows that the massive ions, which become non-magnetized soon after entering the divergent MN, do not follow magnetic lines but instead separate *inward* from the field, even if electrons remain fully-magnetized (except at the plasma edge, where quasineutrality might pull a negligible fraction of the ion flow along with the electrons). This behavior explains the experimental observations<sup>24-26,28</sup> of ion flux tube separation, and follows from the fact that ion momentum increases along the nozzle, while the magnitude of the electric and magnetic forces that try to deflect them outward decreases downstream.

One of the aspects of the expansion that is determinant in the far-region is the rate at which electron cooling takes place. Experimental measurements<sup>14,25</sup> suggest that electron temperature varies only slowly along the near-region, with an 'effective' polytropic exponent between 1 (fully isothermal model) and 1.2. Raadu,<sup>35</sup> on the other hand, predicts an adiabatic cooling of the electrons with a 1D self-similar expansion model, acknowledging that some rethermalization process must exist to explain the near-constant observed temperatures. Following a different approach, Arefiev *et al.*<sup>36</sup> describe the cooling process in transient plasma expansions as the adiabatic reflection of electrons on a rarefaction wave on the plasma front; this explanation, however, seems unsatisfactory for the steady-state, where this moving barrier has reached infinity. At any rate, cooling in the collisionless electron expansion is a non-trivial process, likely involving complex heat

fluxes, potential barriers, and anisotropization<sup>37,38</sup> Additionally, anomalous electron thermodynamics could also explain certain flow structures like weak electric double layers,<sup>39–41</sup> which have been observed in some HPT prototypes.<sup>42</sup>

Another aspect of interest is the distinct roles of electron and ion temperatures,  $T_e$  and  $T_i$ , in the expansion. While measurements indicate that in many cases  $T_i \ll T_e$ , such as in HTPs or ECRTs (and to some extent AF-MPDs too), and therefore many of the existing plasma/MN models disregard ion temperature, this is not the case in other devices such as the VASIMR, where the ion-cyclotron resonance heater deposits most of the applied power directly into ions. Whereas the expansion in the former examples is driven by electron thermal energy (giving rise to the ambipolar acceleration mechanism), it is driven by ion thermal energy in the latter.

In this Paper we perform a first assessment of the effects of electron cooling and ion temperature in the plasma acceleration and plume formation, without inquiring on the physical mechanisms responsible for that cooling (which will be object of future research) or the details of the ion heating process. To this end, our 2D plasma/MN model<sup>20</sup> is extended to treat both the electrons and ions as a hot polytropic species, which can be regarded as an ‘effective’ cooling law. The results will then be compared against the fully isothermal electron and cold ion plasma jet with zero cooling, analyzing the differences found in the behavior of plasma forces, ambipolar electric field, and overall efficiencies. In the absence of a model of the anisotropization of the magnetized electrons or ions, in this preliminary stage we will assume that both populations remain close to Maxwellian as they expand downstream.

The rest of the paper is structured as follows. Next Section briefly introduces the extended model with polytropic electrons and non-zero ion temperature. Electron cooling effects are investigated in Section III. The role of ion temperature is discussed in Section IV. Finally, conclusions of this analysis and an outlook into the next steps to understand the thermodynamics of a plasma in a MN are presented in Section V.

## II. Extended plasma/MN model

A full derivation of the axisymmetric, two-fluid plasma/MN model can be found in Ref. 20; hence, here only a summary is given to facilitate the comprehension of the rest of the paper, and focus is placed on the extension to include electron and ion thermodynamics.

The plasma is assumed collisionless, quasineutral, and globally-current-free. Electrons have negligible inertia and are fully-magnetized, meaning that electron streamtubes are magnetic streamtubes, whereas ions can have any magnetization degree. In this first step towards modeling the evolution of the distribution functions, as a rough approximation both species are considered isotropic and Maxwellian. Under these assumptions, the plasma responds to following equations:

$$\nabla \cdot (n\mathbf{u}_i) = 0 \quad (1)$$

$$\nabla \cdot (n\mathbf{u}_e) = 0, \quad (2)$$

$$m_i (\mathbf{u}_i \cdot \nabla) \mathbf{u}_i = -\nabla(nT_i)/n - e\nabla\phi + e\mathbf{u}_i \times \mathbf{B}, \quad (3)$$

$$0 = -\nabla(nT_e)/n + e\nabla\phi - eu_{\theta e}B\mathbf{1}_{\perp}, \quad (4)$$

where most symbols are conventional, and  $\mathbf{1}_{\perp}$  is a unit vector perpendicular to the magnetic field (so that  $[\mathbf{1}_{\parallel}, \mathbf{1}_{\perp}, \mathbf{1}_{\theta}]$  constitutes a local orthonormal reference system). In the following, the induced magnetic field that the plasma generates is neglected, assuming a low plasma  $\beta$  (although it can be included easily with an iterative approach<sup>43</sup>), keeping only the applied magnetic field, which satisfies  $r\mathbf{B} = \nabla\psi \times \mathbf{1}_{\theta}$ , with  $\psi$  the magnetic streamfunction.

Next, we need a model for  $T_i$ ,  $T_e$ . In the case of electrons, we will assume that they follow a polytropic expansion law,

$$T_e = C_e n^{\gamma_e - 1}, \quad (5)$$

along each magnetic line, where  $\gamma_e$  is an effective specific heat ratio exponent, and  $C_e = T_e(0, r)/[n(0, r)]^{\gamma_e - 1}$  a constant defined by the upstream conditions of that line. Observe that, due to the lack of collisions and the strong magnetization of electrons,  $C_e$  is in principle different for each magnetic line, i.e.,  $C_e = C_e(\psi)$ . Ions, on the other hand, are only marginally magnetized in the envisaged applications. This means that cross-field thermal mixing takes place more easily for ions than for electrons, suggesting the choice of a simple polytropic model for the whole population,

$$T_i = C_i n^{\gamma_i - 1}, \quad (6)$$

with  $C_i = T_{i0}/n_0^{\gamma_i-1}$  given by the values at the origin of coordinates (the central point of the MN throat).

The above model for electrons and ions allows for a convenient mathematical simplification of the equations. First, note that an ion barotropy function exists,

$$h_i = \frac{\gamma_i}{\gamma_i - 1} T_i \quad (7)$$

that satisfies  $dh_i = d(nT_i)/n$  (or  $h_i = T_{i0} \ln(n/n_0)$  in the isothermal limit  $\gamma_i = 1$ ). Then, combining both Eq. (3) and Eq. (4) to eliminate the electric field, the equation for ions becomes

$$m_i (\mathbf{u}_i \cdot \nabla) \mathbf{u}_i = -\nabla(nT_e + nT_i)/n + e\mathbf{u}_i \times \mathbf{B} - eu_{\theta e} B \mathbf{1}_{\perp}, \quad (8)$$

so that Eq. (8) is analogous to the momentum equation for cold ions, when the ‘total’ temperature  $T = T_e + T_i$  is used. Multiplying Eq. (3) by  $\mathbf{u}_i$  and integrating yields the ion energy equation,

$$m_i \frac{\mathbf{u}_i^2}{2} + \int \frac{d(nT_e + nT_i)}{n} = m_i \frac{\mathbf{u}_i^2}{2} + e\phi + h_i = H_i(\psi_i), \quad (9)$$

where  $H_i$  is a constant on each ion streamtube, labeled by  $\psi_i$ .

Examination of these expressions shows that the effective ion sound velocity is given by

$$c_s^2 = \frac{\gamma_e T_e + \gamma_i T_i}{m_i}, \quad (10)$$

which can be used to define the longitudinal ion Mach number  $M$ , given by  $M^2 = (u_{zi}^2 + u_{ri}^2)/c_s^2$ .

Lastly, electron momentum equations can be expressed as the projections of Eq. (4) along  $\mathbf{1}_{\parallel}$  and  $\mathbf{1}_{\perp}$ , which yield, respectively,

$$H_e(\psi) = C_e(\psi) \frac{\gamma_e}{\gamma_e - 1} n^{\gamma_e-1} - e\phi, \quad (11)$$

$$\frac{eu_{\theta e}}{r} = \frac{dC_e}{d\psi} n^{\gamma_e-1} - \frac{dH_e}{d\psi}. \quad (12)$$

Observe that the term  $n^{\gamma_e-1}/(\gamma_e - 1)$  becomes  $\ln(n/n_0)$  in the isothermal electron limit,  $\gamma_e \rightarrow 1$  (save for an additive constant).

Given sufficient upstream conditions, Eq. (11) provides a relation between  $n$  and  $\phi$ , required to solve Eqs. (1) and (3). As the ion flow is sonically choked at the nozzle throat, the ion flow in the divergent MN is supersonic and constitutes an hyperbolic problem susceptible of integration with the method of characteristics. Likewise, Eq. (12) can be used to calculate the Hall velocity  $u_{\theta e}$ . Parallely or afterward, Eq. (2) yields  $u_{\parallel e}$  (after imposing  $u_{\perp e} = 0$ ). Observe that  $u_{\theta e}/r$  is constant along magnetic streamtubes (isorotation) only when  $dC_e/d\psi = 0$ ; otherwise, the first term in the right hand side of Eq. (12) adds a contribution to  $u_{\theta e}/r$ , which decreases to zero as  $n \rightarrow 0$  downstream, where  $eu_{\theta e}/r \rightarrow -dH_e/d\psi$ .

### III. Effects of electron cooling

Equation (11) condenses the effect of electron streamline thermodynamics on the behavior of the ambipolar electric potential,  $\phi$ , from where various aspects can be already inferred. To focus the discussion on the effects of electron cooling, in this section two simulations with plasma conditions  $n(0, r) = n_0$ ,  $C_e(0, r) = C_{e0}$ ,  $\phi(0, r) = 0$ ,  $u_{\theta i}(0, r) = 0$  and  $C_i = 0$  will be used, with two different values of  $\gamma_e$ : 1.2 (moderate cooling rate) and 1 (isothermal electrons). The MN geometry is given by a single current loop located at  $z = 0$ ,  $r = 3.5R$ , where  $R$  is the radius of the plasma jet at the throat, and the magnitude of the magnetic field is fixed at  $eBR/\sqrt{m_i T_{e0}} = 0.1$  (ions essentially unmagnetized).

First, as plotted in Fig. 1, the polytropic cooling law considered here reproduces the existence of an asymptotic value of the potential on each magnetic tube,

$$e\phi \rightarrow e\phi_{\infty} = -\frac{\gamma_e}{\gamma_e - 1} T_{e0}, \text{ as } (n, T_e) \rightarrow 0, \quad (13)$$

with  $T_{e0}$  the value at the throat. Such a bounded potential is an expected feature of the expansion, in contrast to the unphysical behavior in an isothermal model where  $\phi$  continues to decrease logarithmically to infinity.

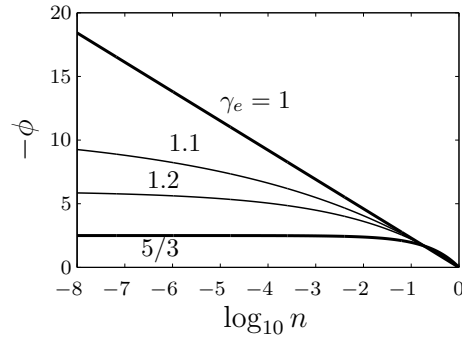


Figure 1. Ambipolar electric potential  $\phi$  as a function of plasma density  $n$ , for different values of  $\gamma_e$ .

As expected, the ion Mach number  $M$  increases at a faster rate than in the isothermal plasma, since  $c_s \propto \sqrt{T_e}$  (Fig. 2). The higher Mach number is more marked at the plasma edge, where the isothermal plasma reaches only half that value. In contrast,  $u_i \propto \sqrt{-\phi}$  is lower when plasma cooling takes place than in the isothermal model. Interestingly, the difference in velocity magnitude between jet edge and axis is also reduced, and in the present simulations, where  $\phi_\infty$  is the same for all magnetic lines, must asymptotically vanish. The higher Mach numbers mean that the plasma becomes hypersonic at an earlier stage, and pressure and electric forces become negligible much sooner, thus affecting the development of the plume in the far region. As the forces that deflect ions radially outward are lower compared to ion inertia, this in turn leads to a less divergent plasma plume (i.e., a more collimated jet).

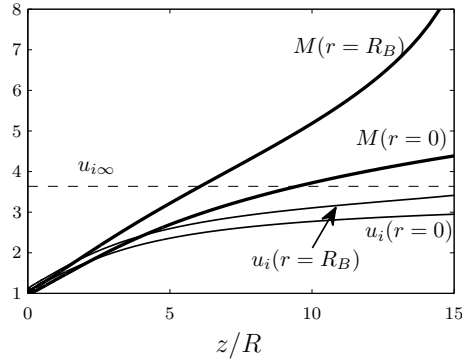
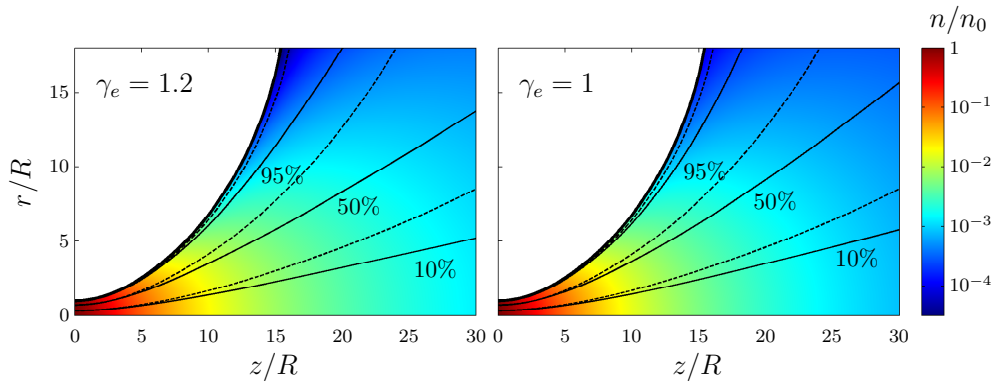


Figure 2. Plasma Mach number (thick lines) and ion velocity  $u_i$  (thin lines) along the MN axis ( $r = 0$ ) and plasma edge ( $R_B$ ) for  $\gamma_e = 1.2$ . The asymptotic ion velocity for a complete expansion,  $u_{i\infty} = \sqrt{-2\phi_\infty/m_i + u_{i0}^2}$  is shown as a dashed line. Ion velocities are non-dimensionalized with  $\sqrt{T_{e0}/m_i}$  (not the sonic velocity).

The lower divergence of ion streamlines can be observed in Fig. 3, compared to the  $\gamma_e = 1$  (isothermal) case. This increased inward ion separation from magnetic streamlines leads to a larger radial density gradient and an enhanced plume divergence efficiency  $\eta_{plume}$  (shown in Fig. 4), defined as the ratio of axial to total ion kinetic power at a given  $z = \text{const}$  section.<sup>20</sup>

In relation to this, plasma cooling facilitates plasma detachment. To justify this statement, observe that ion detachment from the MN is guaranteed as soon as they become unmagnetized (which occurs soon after the MN throat in practical devices) and hypersonic,<sup>34</sup> since magnetic, electric, and pressure forces on them decrease while their inertia increases, meaning that eventually no further outward deflection can occur and their trajectories will approach a straight line, i.e., most ions do not turn around, even if electrons remain magnetized. As ions carry the plasma mass flow, their detachment ensures the ejection of the propellant mass as required for propulsion. This of course gives rise to longitudinal electric currents, which need to find a closure outside of the present model, both upstream (inside the plasma source) and downstream (once electrons demagnetize, too). The electron flux on each magnetic tube, uncoupled from the ion flux (except to ensure the global current-free condition of the jet), is expected to adapt to minimize the longitudinal electric currents. Notice nonetheless that ion inward separation is a robust feature of the MN flow, essentially



**Figure 3.** Plasma density (background map) for  $\gamma_e = 1.2$  (left) and  $\gamma_e = 1$  (right), with the ion streamtubes (solid) and the corresponding magnetic/electron streamtubes (dashed).

unaffected by the presence and closure of these currents.

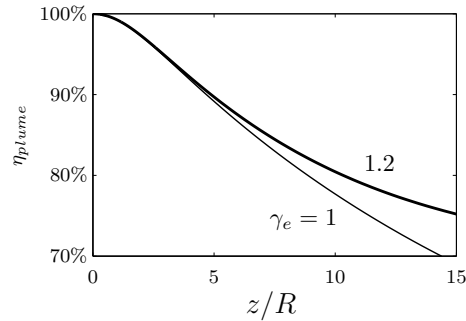


**Figure 4.** Plume divergence efficiency  $\eta_{plume} = P_{iz}/P_i$  (ratio of axial to total ion power) for  $\gamma_e = 1.2$  (thick line) and 1 (thin line).

Lastly, the existence of an asymptotic value of the electric potential helps to find a clean closure for the energy balance in the plasma plume. In essence, electron cooling at a different rate than the adiabatic one,  $\gamma_e = 5/3$ , is sustained by an electron heat flux  $q_{\parallel e}$  coming from the plasma source that keeps up the electron temperature up as they expand; i.e., if the electrons cool down as  $T_e \propto n^{\gamma_e - 1}$  instead of cooling down as  $T_e \propto n^{2/3}$ , the excess power needed to replenish their internal energy is provided by  $-\partial q_{\parallel e}/\partial \mathbf{1}_{\parallel}$ . Assuming that the plasma completes the expansion within the region of validity of the model, and that  $q_{\parallel e} = 0$  there (i.e., when  $\phi = \phi_{\infty}$ ), we can estimate  $q_{\parallel e}$  at the MN throat from the energy equation. For the sake of illustration, integrating between the throat and the asymptotic expansion state in the example simulations yields (observe that more complex initial conditions with  $C_e(\psi) \neq \text{const}$  will complicate this analysis)

$$P_{beam} = \dot{m}_i \left( \frac{u_{i0}^2}{2} + \frac{5 T_{e0}}{2 m_i} \right) + Q_e(0) = \dot{m}_i \left( \frac{u_{i0}^2}{2} + \frac{\gamma_e T_{e0}/m_i}{\gamma_e - 1} \right) \quad (14)$$

where  $Q_e(z)$  is the integrated electron heat flux at section  $z$ . This equation provides the total power of the beam,  $P_{beam}$ , flowing out of the plasma source, which is required to compute the efficiency of the plasma thruster as a whole.<sup>44</sup> The total electron heat flux at the throat,

$$Q_e(0) = \frac{3 \dot{m}_i T_{e0}}{2 m_i} \left( \frac{5/3 - \gamma_e}{\gamma_e - 1} \right), \quad (15)$$

has been plotted in Fig. 5 as a function of  $\gamma_e$ , stressing the need to have an accurate electron cooling model (alternatively, an ‘‘effective’’ cooling exponent  $\gamma_e$ ) to calculate the efficiency of the device. Experimental evidence<sup>14,25</sup> seems to suggest that  $\gamma_e < 5/3$ , closer to the isothermal than to the adiabatic limit (at least in the near MN region), so that  $Q_e(0)$  is expected to be non-zero. Observe however that a ‘complete expansion’ state does not exist in the isothermal model, which nonphysically leads to infinite values of  $q_{\parallel e}$ .

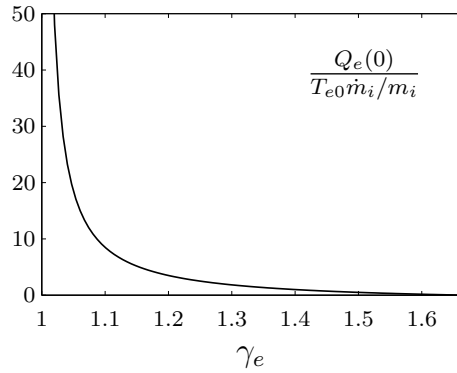


Figure 5. Non-dimensional electron heat flux at the nozzle throat flowing out of the plasma source as a function of  $\gamma_e$ .

#### IV. Influence of ion thermal energy

Both ion and electron thermal energy can be transformed into directed axial ion energy in the MN: in essence, the perpendicular energy of each charged particle is converted into parallel energy thanks to the inverse magnetic mirror effect. Notwithstanding, the macroscopic role of each species thermal energy is different. Electron thermal energy, on the one hand, causes electrons to expand and to create an ambipolar electric field that pulls ions downstream.<sup>20</sup> In this way, the internal electric field  $-\nabla\phi$  acts as the intermediary for the plasma energy conversion. On the other hand, ion thermal energy is responsible for the direct gasdynamic acceleration mechanism, which takes place without the mediation of the electric field.

In an actual plasma thruster, thermal energy is divided between ions and electrons, although usually not evenly. This means that both acceleration mechanisms, ambipolar and gasdynamic, will coexist; the relevance of each of them depends on the fraction of thermal energy carried by each species, measured by the parameter  $T_{i0}/T_{e0}$ . In some devices like the HPT,  $T_{i0}/T_{e0} \ll 1$ , suggesting that ion temperature can be safely neglected on a first analysis. On the contrary, the operation of other thrusters under development, such as the VASIMR, which incorporates an ion cyclotron resonance heater to increase the energy of the plasma after ionization in the source, deposit most of the energy on the ions, which can reach values of  $T_{i0}/T_{e0} = O(1)-O(10)$ . The dominant part of the ion internal energy in this case is collimated in the perpendicular direction in the gyromotion of ions, which have a marked non-isotropic distribution.

The ambipolar and gasdynamic acceleration mechanisms are compared in Fig. 6 for  $T_{i0}/T_{e0} = 5$ ,  $\gamma_i = 5/3$ ,  $\gamma_e = 1$ , and an initially uniform plasma profile with  $n = n_0$  and  $u_{\theta i} = 0$  at the throat. This example intends to illustrate a possible scenario in which ion temperature evolves nearly adiabatically, while electrons are close to isothermal; the inclusion of ion internal energy in this way is a simple, preliminary approach to the study of more complex ion populations, such as in the aforementioned VASIMR. Clearly, in this case, due to the different cooling rates of each species, the weight of the gasdynamic mechanism is largest near the MN throat, where  $T_i$  is high, accounting for nearly five sixths of the total acceleration. As the expansion proceeds downstream, however, the ion population cools down faster than the electrons, and the gasdynamic mechanism loses importance in favor for the ambipolar one. This is observed in the lower fraction of the total acceleration caused by ion thermal energy. Eventually, ions must cool down and the residual acceleration is caused only by the ambipolar electric field set up by the electrons.

Dominant ion thermal energy in the model also poses several questions on how the perpendicular confinement of that energy by the MN takes place. This can be better understood by analyzing the radial plasma balance at the MN throat. In the case of magnetized electrons, they are effectively confined by the magnetic field: the gyration of each electron about its magnetic line adds up to give rise to the azimuthal diamagnetic drift, which sets up a radial force balance at the throat:  $\partial p / \partial r \equiv -en u_{\theta e, diam} B$ . In contrast, heavier ions are typically unmagnetized, meaning that we cannot count on magnetic forces to control the perpendicular expansion of the ion population. Indeed, the expected scenario is that ions are confined by a radial electric field  $-\partial\phi/\partial r = \partial p_i/\partial r$  set up by the electrons as the ions pull outward, while the ion azimuthal velocity remains negligibly low. This, in turn, increases the demand on electron azimuthal velocity, which must now confine themselves and the ions too, and an additional drift  $u_{\theta e, E \times B} \equiv -(\partial\phi/\partial r)/B$  occurs. The

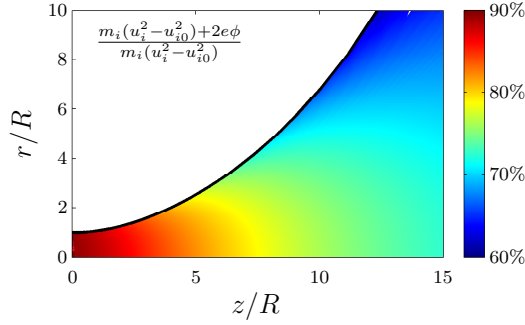


**Figure 6.** Fraction of the total ion kinetic energy gain,  $m_i(u_i^2 - u_{i0}^2)/2$ , afforded by the ion thermal energy, giving rise to the direct gasdynamic acceleration mechanism.

summation of both drifts,  $u_{\theta e, diam}$  and  $u_{\theta e, E \times B}$ , gives the total electron azimuthal velocity at the throat,  $u_{\theta e}$ , for the plasma force balance there. In an initially non-uniform plasma profile,  $u_{\theta e}$  exists as a function of  $\partial(p_e + p_i)/\partial r$ ; in an initially uniform plasma, however, all the gradients (and the  $u_{\theta e}$ ) concentrate in a thin layer at the jet edge,<sup>20</sup> of a thickness in the order of  $O(\ell_e)$ , the electron Larmor radius.

This means that the map of the electric field in the divergent MN depends on the ion thermal energy too, and in particular, is affected by the  $T_i/T_e$  ratio. To illustrate this effect, Fig. 7 presents, for different values of  $T_{i0}/T_{e0}$ , the electric potential for the plasma jet with an initially non-uniform profile with  $n = J_0(a_0 r/R)$  and  $u_{\theta i} = 0$ , where  $J_0$  is the Bessel function of the first kind of order 0, and  $a_0$  is its first zero. For simplicity, both ions and electrons have been considered isothermal here. As it can be seen in the curvature of the isopotential lines in Fig. 7, the ambipolar electric potential decreases monotonically downstream and outward only when  $T_{i0}/T_{e0} = 0$ ; in any other situations,  $-\partial\phi/\partial r$  points inward initially, in the neighborhood of the throat, to confine the radial expansion of ions, and later downstream  $-\partial\phi/\partial r$  points outward again. As  $T_{i0}/T_{e0}$  is increased, this effect becomes stronger, extending further downstream, and the potential jump experimented by the plasma (normalized with the ‘total’ temperature  $T = T_i + T_e$ ) decreases.

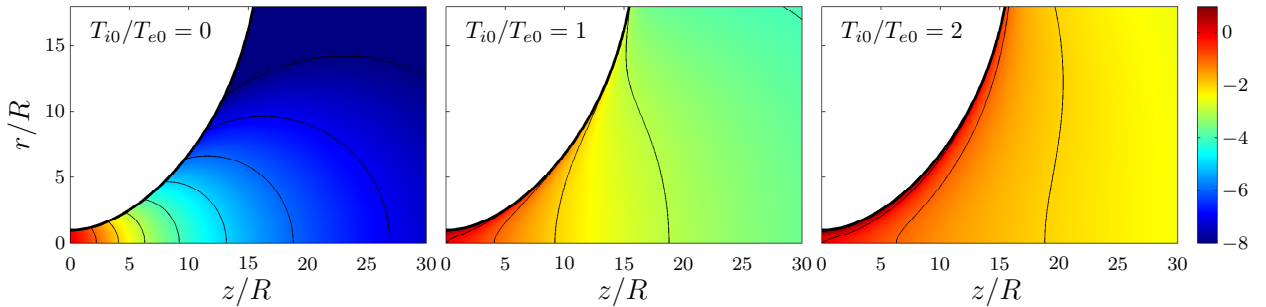


**Figure 7.** Electric potential  $\phi$  for  $T_{i0}/T_{e0} = 0, 1$  and  $2$ , for an initially non uniform plasma jet. The electric potential has been normalized with the ‘total’ temperature  $T = T_e + T_i$ . Solid lines represent isopotential surfaces in the plasma, spaced in increments of  $e\Delta\phi/T = 1$ .

## V. Conclusion and future work

In the present paper we have extended our 2D plasma/MN model<sup>20</sup> to include simple thermodynamic models for electrons and ions, as a first stage to understand the effects of electron cooling and ion thermal energy on the expansion.

Electron cooling, while elusive to detection in some experiments, is expected to occur in the MN far-region as the plasma continues to expand, leading to an asymptotic value of the electric potential, absent in isothermal models. Further work must identify the exact mechanisms that enable a magnetized, collisionless electron population to cool down, and assess the heat fluxes along the magnetic field. Observe that the



complexity of the thermodynamic behavior of electrons and ions in MN-based devices will demand advanced models, taking into account kinetic considerations. A proper cooling model will also address the non-isotropization of the species downstream, and allow for inclusion of collisions with the jet plasma and with the ambient plasma. The polytropic model described here, while unable to reproduce these phenomena, can be regarded as a simplified tool to study the consequences of an ‘effective’ cooling, once that  $\gamma_e$  is known or estimated by other means. Extension to spatially varying  $\gamma_e$  is straightforward.

In regard to ions, inclusion of their thermal energy in the model allows to investigate the combined gasdynamic and ambipolar acceleration mechanisms. Again, the ability to include non-isotropic populations is deemed an important aspect, which will be object of future work. A detailed model of the kinetic evolution of the ion species is particularly relevant to high-ion-energy devices such as the VASIMR, where the inverse magnetic mirror effect on ions is one of the dominant acceleration mechanisms. The existence of dominant ion thermal energy raises questions on the structure of the electric field and the radial balance of the plasma at the MN throat. These aspects are intimately linked to the plasma generation conditions in the upstream source, and therefore further study of these conditions in different plasma thrusters is also required.

## Acknowledgments

This work is sponsored by the Spanish R & D National Plan (Project AYA-2010-61699). The authors thank M. Martínez-Sánchez and J. Navarro-Cavallé for the insightful discussions on electron cooling mechanisms.

## References

- <sup>1</sup>Ziemba, T., Carscadden, J., Slough, J., Prager, J., and Winglee, R., “High Power Helicon Thruster,” *41th Joint Propulsion Conference*, 2005.
- <sup>2</sup>Batishchev, O., “Minihelicon Plasma Thruster,” *IEEE Transaction on Plasma Science*, Vol. 37, 2009, pp. 1563–1571.
- <sup>3</sup>Charles, C., Boswell, R., and Lieberman, M., “Xenon ion beam characterization in a helicon double layer thruster,” *Applied Physics Letters*, Vol. 89, 2006, pp. 261503.
- <sup>4</sup>Pavarin, D., Ferri, F., Manente, M., Curreli, D., Guclu, Y., Melazzi, D., Rondini, D., Suman, S., Carlsson, J., Bramanti, C., Ahedo, E., Lancellotti, V., Katsonis, K., and Markelov, G., “Design of 50W Helicon Plasma Thruster,” *31th International Electric Propulsion Conference*, IEPC 2009-205, 2009.
- <sup>5</sup>Sercel, J. C., “Electron-cyclotron-resonance (ECR) plasma acceleration,” *AIAA 19th Fluid Dynamics, Plasma Dynamics and Lasers Conference*, 1987.
- <sup>6</sup>Krülle, G., Auweter-Kurtz, M., and Sasoh, A., “Technology and application aspects of applied field magnetoplasmadynamic propulsion,” *J. Propulsion and Power*, Vol. 14, 1998, pp. 754–763.
- <sup>7</sup>Tikhonov, V., Semenikhin, S., Brophy, J., and Polk, J., “Performance of 130kW MPD thruster with an external magnetic field and Li as a propellant,” *Proceedings of the 25 th International Electric Propulsion Conference*, 1997, pp. 728–733.
- <sup>8</sup>Tang, H.-B., Cheng, J., Liu, C., and York, T. M., “Study of applied magnetic field magnetoplasmadynamic thrusters with particle-in-cell and Monte Carlo collision. II. Investigation of acceleration mechanisms,” *Physics of Plasmas*, Vol. 19, 2012, pp. 073108.
- <sup>9</sup>Diaz, F., Squire, J., Bengtson, R., Breizman, B., Baity, F., and Carter, M., “The Physics and Engineering of the VASIMR Engine,” *36th AIAA/ASME/SAE/ASEE Joint Propulsion Conference & Exhibit*, AIAA 2000-3756, 2000.
- <sup>10</sup>Navarro, J., Ahedo, E., Merino, M., Gómez, V., and Ruiz, M., “Helicon Plasma Thrusters: prototypes and advances on modeling,” *33rd International Electric Propulsion Conference*, No. IEPC-2013-285, Electric Rocket Propulsion Society, Fairview Park, OH, 2013.
- <sup>11</sup>Andersen, S., Jensen, V., Nielsen, P., and D’Angelo, N., “Continuous Supersonic Plasma Wind Tunnel,” *Phys. Fluids*, Vol. 12, 1969, pp. 557–560.
- <sup>12</sup>Kuriki, K. and Okada, O., “Experimental Study of a Plasma Flow in a Magnetic Nozzle,” *Physics of Fluids*, Vol. 13, 1970, pp. 2262.
- <sup>13</sup>York, T. M., Jacoby, B. A., and Mikellides, P., “Plasma flow processes within magnetic nozzle configurations,” *Journal of Propulsion and Power*, Vol. 8, No. 5, 1992, pp. 1023–1030.
- <sup>14</sup>Inutake, M., Ando, A., Hattori, K., Tobari, H., and Yagai, T., “Characteristics of a Supersonic Plasma Flow in a Magnetic Nozzle,” *J. Plasma Fusion Res.*, Vol. 78, 2002, pp. 1352–1360.
- <sup>15</sup>Kosmahl, H., “three-dimensional plasma acceleration through axisymmetric diverging magnetic fields based on dipole moment approximation,” Tech. rep., NASA TN D-3782, 1967.
- <sup>16</sup>Chubb, D. L., “Fully ionized quasi-one-dimensional magnetic nozzle flow,” *AIAA Journal*, Vol. 10, No. 2, 1972, pp. 113–114.
- <sup>17</sup>Gerwin, R., Marklin, G., Sgro, A., and Glasser, A., “Characterization of plasma flow through magnetic nozzles,” Tech. Rep. AFSOR AL-TR-89-092, Los Alamos National Laboratory, 1990.
- <sup>18</sup>Sercel, J., “Simple model of plasma acceleration in a magnetic nozzle,” *21st International Electric Propulsion Conference*, Vol. 1, 1990.

- <sup>19</sup>Mikellides, P., Turchi, P., and Roderick, N., “Applied-field magnetoplasmadynamic thrusters, Part 1: Numerical simulations using the MACH2 code,” *Journal of Propulsion and Power*, Vol. 16, No. 5, 2000.
- <sup>20</sup>Ahedo, E. and Merino, M., “Two-dimensional supersonic plasma acceleration in a magnetic nozzle,” *Physics of Plasmas*, Vol. 17, 2010, pp. 073501.
- <sup>21</sup>Roberson, B., Winglee, R., and Prager, J., “Enhanced diamagnetic perturbations and electric currents observed downstream of the high power helicon,” *Physics of Plasmas*, Vol. 18, 2011, pp. 053505.
- <sup>22</sup>Takahashi, K., Lafleur, T., Charles, C., Alexander, P., Boswell, R. W., et al., “Axial force imparted by a current-free magnetically expanding plasma,” *Physics of Plasmas*, Vol. 19, No. 8, 2012, pp. 083509.
- <sup>23</sup>Gerwin, R. A., “Integrity of the plasma magnetic nozzle,” Tech. rep., NASA/TP—2009-213439, 2009.
- <sup>24</sup>Cox, W., Charles, C., Boswell, R., and Hawkins, R., “Spatial retarding field energy analyzer measurements downstream of a helicon double layer plasma,” *Applied Physics Letters*, Vol. 93, 2008, pp. 071505.
- <sup>25</sup>Deline, C., Bengtson, R., Breizman, B., Tshentsov, M., Jones, J., Chavers, D., Dobson, C., and Schuettelpelz, B., “Plume detachment from a magnetic nozzle,” *Physics of Plasmas*, Vol. 16, 2009, pp. 033502.
- <sup>26</sup>Terasaka, K., Yoshimura, S., Ogiwara, K., Aramaki, M., and Tanaka, M., “Experimental studies on ion acceleration and stream line detachment in a diverging magnetic field,” *Physics of plasmas*, Vol. 17, 2010, pp. 072106.
- <sup>27</sup>Squire, J. P., Olsen, C. S., Chang-Díaz, F. R., Cassady, L. D., Longmier, B. W., Ballenger, M. G., Carter, M. D., Glover, T. W., and McCaskill, G. E., “VASIMR VX-200 Operation at 200 kW and Plume Measurements: Future Plans and an ISS EP Test Platform,” *32nd International Electric Propulsion Conference*, 2011.
- <sup>28</sup>Takahashi, K., Itoh, Y., and Fujiwara, T., “Operation of a permanent-magnets-expanding plasma source connected to a large-volume diffusion chamber,” *Journal of Physics D: Applied Physics*, Vol. 44, 2011, pp. 015204.
- <sup>29</sup>Moses, R., Gerwin, R., and Schoenberg, K., “Resistive plasma detachment in nozzle based coaxial thrusters,” *Proceedings Ninth Symposium on Space Nuclear Power Systems, Albuquerque, New Mexico, 1992*, AIP Conference Proceedings No. 246, 1992, pp. 1293–1303.
- <sup>30</sup>Hooper, E., “Plasma Detachment from a Magnetic Nozzle,” *Journal of Propulsion and Power*, Vol. 9, No. 5, 1993, pp. 757–763.
- <sup>31</sup>Arefiev, A. and Breizman, B., “Magnetohydrodynamic scenario of plasma detachment in a magnetic nozzle,” *Physics of Plasmas*, Vol. 12, 2005, pp. 043504.
- <sup>32</sup>Ahedo, E. and Merino, M., “On plasma detachment in propulsive magnetic nozzles,” *Physics of Plasmas*, Vol. 18, 2011, pp. 053504.
- <sup>33</sup>Ahedo, E. and Merino, M., “Two-dimensional plasma expansion in a magnetic nozzle: separation due to electron inertia,” *Physics of Plasmas*, Vol. 19, 2012, pp. 083501.
- <sup>34</sup>Merino, M. and Ahedo, E., “Magnetic Nozzle Far-Field Simulation,” *48<sup>th</sup> AIAA/ASME/SAE/ASEE Joint Propulsion Conference & Exhibit*, No. AIAA-2012-3843, AIAA, Washington DC, 2012.
- <sup>35</sup>Raadu, M. A., “Expansion of a plasma injected from an electrodeless gun along a magnetic field,” *Plasma Physics*, Vol. 21, No. 4, 1979, pp. 331.
- <sup>36</sup>Arefiev, A. and Breizman, B., “Ambipolar acceleration of ions in a magnetic nozzle,” *Physics of Plasmas*, Vol. 15, 2008, pp. 042109.
- <sup>37</sup>Egedal, J., Le, A., and Daughton, W., “A review of pressure anisotropy caused by electron trapping in collisionless plasma, and its implications for magnetic reconnection,” *Physics of Plasmas*, Vol. 20, 2013, pp. 061201.
- <sup>38</sup>Martínez-Sánchez, M. and Navarro-Cavallé, J., private communication, 2013.
- <sup>39</sup>Bezzerrides, B., Forslund, D., and Lindman, E., “Existence of rarefaction shocks in a laser-plasma corona,” *Physics of Fluids*, Vol. 21, 1978, pp. 2179.
- <sup>40</sup>Ahedo, E. and Martínez-Sánchez, M., “Theory of a Stationary Current-Free Double Layer in a Collisionless Plasma,” *Physical Review Letters*, Vol. 103, Sep 2009, pp. 135002.
- <sup>41</sup>Merino, M. and Ahedo, E., “Two-dimensional quasi-double-layers in two-electron-temperature, current-free plasmas,” *Physics of Plasmas*, Vol. 20, 2013, pp. 023502.
- <sup>42</sup>Charles, C. and Boswell, R., “Current-free double-layer formation in a high-density helicon discharge,” *Applied Physics Letters*, Vol. 82, 2003, pp. 1356.
- <sup>43</sup>Merino, M. and Ahedo, E., “Plasma detachment mechanisms in a magnetic nozzle,” *47<sup>th</sup> AIAA/ASME/SAE/ASEE Joint Propulsion Conference & Exhibit*, No. AIAA-2011-5999, AIAA, Washington DC, 2011.
- <sup>44</sup>Ahedo, E. and Navarro-Cavallé, J., “Helicon thruster plasma modeling: Two-dimensional fluid-dynamics and propulsive performances,” *Physics of Plasmas*, Vol. 20, 2013, pp. 043512.